Subcarrier and Resource Allocation in Aerial Intelligent Reflecting Surface-Assisted Wireless Networks

Ahmad Kasaeyan*, Minh Dat Nguyen†, Wei-Ping Zhu*, and Wessam Ajib†
*Concordia University and †University of Quebec at Montreal,
*a_kasaey@live.concordia.ca, †nguyen.minh_dat@uqam.ca, *weiping@ece.concordia.ca, and †ajib.wessam@uqam.ca

***Abstract*—This paper addresses the problem of resource allocation in aerial intelligent reflecting surface (AIRS)-assisted wireless networks, where intelligent reflecting surfaces (IRS) are deployed on flying platforms. Specifically, we investigate the joint optimization of AIRS placement and phase shifts, along with base station subcarrier and power allocation to maximize the system sum rate. To address the problem's non-convexity, an alternating optimization framework is proposed. In this framework, we employ K-means clustering to determine optimal AIRS locations and decompose the problem into two interdependent subproblems: AIRS phase optimization on the one hand and base station subcarrier and power allocation on the other hand, each solved iteratively until convergence is reached. In addition, the successive convex approximation method is used to tackle the non-convexity of AIRS phase shift optimization. Numerical results demonstrate that the proposed approach outperforms benchmark schemes, highlighting the potential of AIRS to extend cellular coverage in challenging scenarios such as emergencies or regions with limited infrastructure.**

***Index Terms*—aerial intelligent reflecting surface (AIRS), resource allocation, alternating optimization**

I. Introduction

Advancements in wireless communication have increased demand for innovative solutions to address challenges in coverage, capacity, and spectral efficiency. Among these solutions, Intelligent Reflecting Surfaces (IRS) and Unmanned Aerial Vehicles (UAVs) are promising technologies to enhance the performance of next-generation networks [1]. UAVs deployed as base stations (UAV-BSs) provide a flexible and cost-effective solution for the delivery of wireless communication services, particularly in scenarios where traditional ground-based infrastructure is either infeasible or inefficient [2]. Moreover, by taking advantage of advanced technologies such as millimeter wave (mmWave) communication and beamforming, UAV platforms can significantly improve the achievable sum rate for users [3].

The integration of IRS with UAV-aided networks significantly improves both the average achievable rate and the overall communication performance in air-ground networks [4]. For example, [5] investigates sum rate maximization in IRS-assisted UAV with Orthogonal Frequency Division Multiple Access (OFDMA) communication systems, illustrating how the synergy between IRS and UAV can improve communication efficiency and optimize network performance. Similarly, [6] explores the potential of IRS integration in enhancing multi-UAV Non-Orthogonal Multiple Access (NOMA) networks, to improve communication capacity and system performance.

By deploying IRS on aerial platforms like UAVs, the system can benefit from greater deployment flexibility and a broader range of signal reflections compared to fixed installations. Aerial intelligent reflecting surface (AIRS) systems can enhance communication performance by optimizing AIRS trajectory, transmit beamforming, and AIRS phase shifts [7]. Additionally, they strengthen communication security by maximizing secrecy rate through the joint optimization of UAV trajectory, power control, and IRS phase shifts, effectively countering eavesdropping threats. The challenges of balancing mobility, signal reflection, and power efficiency in AIRS systems are partially addressed in [8], providing valuable insights into how AIRS cooperation can maximize the sum rate and enhance communication reliability under covert constraints.

The study in [9] focuses on multi-UAV IRS-assisted communications, specifically addressing multi-node channel modeling and fair sum rate optimization through Deep Reinforcement Learning (DRL). However, it is important to note that this paper does not consider subcarrier scheduling and optimization, which could further impact overall system performance. Similarly, [10] investigates the joint optimization of single AIRS placement and IRS phase shifts in downlink networks, but it does not explore the complexities of user scheduling or multi-UAV scenarios. Furthermore, the authors in [11] explore AIRS communications within a massive Multiple Input Multiple Output (MIMO) system framework, showing the potential of these technologies to enhance communication capacity and reliability. Despite these advancements, a comprehensive understanding of how to effectively integrate multi-UAV IRS systems into OFDMA networks remains an open challenge.

Thus, this paper aims to investigate multi-AIRS communication systems specifically within the OFDMA framework and explore optimization strategies to enhance spectral efficiency while addressing the unique challenges presented by this advanced communication paradigm. The main novelty and technical contribution of this paper is the presentation of an integrated framework for multi-AIRS-assisted OFDMA networks that jointly considers AIRS placement, subcarrier and power allocation, and AIRS phase shift design — aspects which, to the best of our knowledge, have not been addressed

979-8-3503-9281-4/25/$31.00 ©2025 IEEE

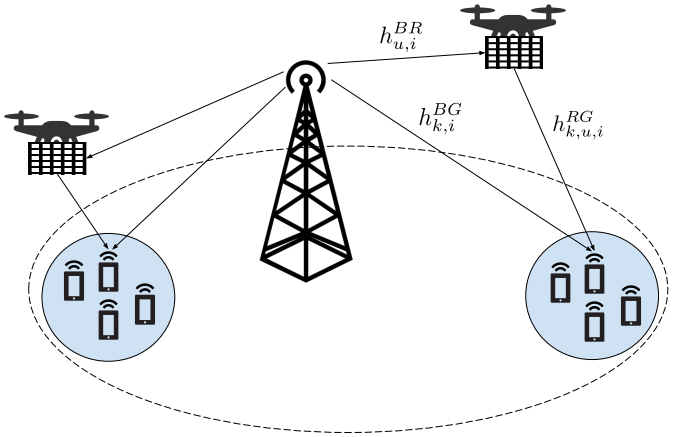

Fig. 1. System model of AIRS-assisted communications.

together in prior works. We first apply a K-means clustering algorithm to determine AIRS locations by grouping users, ensuring efficient deployment and reduced path loss. We then formulate a joint optimization problem of subcarrier scheduling, power allocation, and AIRS phase shifts to maximize spectral efficiency. To handle the complexity, we propose an iterative framework that decouples the problem into subproblems, enabling efficient computation and convergence. Simulation results show that AIRS integration significantly improves spectral efficiency, with 2-bit quantization achieving near-ideal performance and 1-bit quantization providing a simpler yet effective alternative. These findings highlight the potential of AIRS systems to enhance OFDMA networks while balancing performance and implementation complexity.

II. System Model

We consider a downlink network assisted by IRS units mounted on aerial platforms as illustrated in Fig. 1. This model includes a single antenna base station (BS), K users, and U AIRS units. The BS is located at $q^B = [x_B, y_B, z_B]$, while the K users are randomly distributed throughout the service area, with the position of the k-th user denoted by $q_k^G = [x_k, y_k, z_k]$.

Each AIRS unit is equipped with $M = N^2$ reflecting elements, arranged as an $N \times N$ uniform planar array (UPA) with inter-element spacing d in both rows and columns. These elements reflect the signals from the BS toward users, enhancing both coverage and network performance by effectively extending the communication range. We assume that K users are divided into U groups, each group being served exclusively by an AIRS unit. The location of the u-th AIRS is indicated by $q_u^R = [x_u, y_u, z_u]$, where $u = 1, 2, \ldots, U$. The IRS phase shift matrix is denoted by $\Theta_u = \mathrm{diag}(\theta_u)$, with $\theta_u = \left[e^{j\theta_{u,1}}, e^{j\theta_{u,2}}, \ldots, e^{j\theta_{u,M}}\right]^T$, where $\theta_{u,m}$ corresponds to the phase shift applied by the m-th reflecting element of the u-th AIRS, enabling the reflected signals to be steered toward the intended users for improved communication performance.

A. Channel Model

This paper assumes that the total available bandwidth B of the system is divided into I subcarriers, each with a bandwidth of Δf. To mitigate interference and for simplicity, we assume that each subcarrier is exclusively assigned to a single user. The channel model for the proposed system is presented below. Given that the AIRS operates at a higher altitude, the signal propagation link can be effectively modeled as LOS. For the u-th AIRS on the i-th subcarrier, the BS-to-AIRS channel $h_{u,i}^{BR} \in \mathbb{C}^{M\times 1}$ is expressed as

$$h_{u,i}^{BR} = \sqrt{\frac{\beta}{(d_u^{BR})^2}} e^{-j2\pi d_u^{BR} \frac{i\Delta f}{c}} \tag{1}$$
$$\times \left[1, e^{-j\frac{2\pi d}{\lambda}\sin\phi_u^{BR}\cos\xi_u^{BR}}, \ldots, e^{-j\frac{2\pi d(N-1)}{\lambda}\sin\phi_u^{BR}\cos\xi_u^{BR}}\right]^T$$
$$\otimes \left[1, e^{-j\frac{2\pi d}{\lambda}\sin\phi_u^{BR}\sin\xi_u^{BR}}, \ldots, e^{-j\frac{2\pi d(N-1)}{\lambda}\sin\phi_u^{BR}\sin\xi_u^{BR}}\right]^T$$

where β denotes the channel gain at the reference distance of 1 meter, $d_u^{BR} = \|q^B - q_u^R\|$ is the distance between the BS and the u-th AIRS, c denotes the speed of light, f_c is the carrier frequency, and $\lambda = c/f_c$ is the carrier wavelength. Furthermore, ϕ_u^{BR} and ξ_u^{BR} are the vertical and horizontal angles of arrival (AoA) between the BS and the u-th AIRS, with

$$\sin(\phi_u^{BR}) = \frac{z_u - z_B}{d_u^{BR}}, \tag{2}$$
$$\cos(\xi_u^{BR}) = \frac{y_u - y_B}{\sqrt{(x_u - x_B)^2 + (y_u - y_B)^2}}, \tag{3}$$
$$\sin(\xi_u^{BR}) = \frac{x_u - x_B}{\sqrt{(x_u - x_B)^2 + (y_u - y_B)^2}}. \tag{4}$$

On the other hand, due to the assumption of an urban environment and the presence of obstacles, the channel between the u-th AIRS and the k-th user, $h_{k,u,i}^{RG} \in \mathbb{C}^{M\times 1}$, and the direct link between the BS and the k-th user, $h_{k,i}^{BG} \in \mathbb{C}^{1\times 1}$, are modeled by Rician fading as follows:

$$h_{k,i}^{BG} = \sqrt{\frac{\beta}{(d_k^{BG})^\alpha}} \left[\sqrt{\frac{\mathcal{K}}{1+\mathcal{K}}}\bar{h}_{k,i}^{BG} + \sqrt{\frac{1}{1+\mathcal{K}}}\tilde{h}_{k,i}^{BG}\right], \tag{5}$$
$$h_{k,u,i}^{RG} = \sqrt{\frac{\beta}{(d_{k,u}^{RG})^{\alpha'}}} \left[\sqrt{\frac{\mathcal{K}'}{1+\mathcal{K}'}}\bar{h}_{k,u,i}^{RG} + \sqrt{\frac{1}{1+\mathcal{K}'}}\tilde{h}_{k,u,i}^{RG}\right] \tag{6}$$

where $d_{k,u}^{RG} = \|q_u^R - q_k^G\|$ and $d_k^{BG} = \|q^B - q_k^G\|$ are the distances between the u-th AIRS and the k-th user, and the BS and the k-th user, respectively. The parameters (α, α') represent the path loss exponents, and $(\mathcal{K}, \mathcal{K}')$ are the Rician factors for the BS-to-user and AIRS-to-user links, respectively. The non-line-of-sight (NLOS) components $\tilde{h}_{k,i}^{BG} \sim \mathcal{CN}(0,1)$ and $\tilde{h}_{k,u,i}^{RG} \sim \mathcal{CN}(0,1)$ correspond to Rayleigh fading.

The line-of-sight (LOS) components are expressed as

$$\bar{h}_{k,i}^{BG} = e^{-j2\pi d_k^{BG} \frac{i\Delta f}{c}}, \tag{7}$$

$$\bar{h}_{k,u,i}^{RG} = e^{-j2\pi d_{k,u}^{RG} \frac{i\Delta f}{c}} \tag{8}$$
$$\times \left[1, e^{-j\frac{2\pi d}{\lambda}\sin\phi_{k,u}^{RG}\cos\xi_{k,u}^{RG}}, \ldots, e^{-j\frac{2\pi d(N-1)}{\lambda}\sin\phi_{k,u}^{RG}\cos\xi_{k,u}^{RG}}\right]^T$$
$$\otimes \left[1, e^{-j\frac{2\pi d}{\lambda}\sin\phi_{k,u}^{RG}\sin\xi_{k,u}^{RG}}, \ldots, e^{-j\frac{2\pi d(N-1)}{\lambda}\sin\phi_{k,u}^{RG}\sin\xi_{k,u}^{RG}}\right]^T$$

where $\sin(\phi_{k,u}^{RG}) = \frac{z_u - z_k}{d_{k,u}^{RG}}$, $\cos(\xi_{k,u}^{RG}) = \frac{y_u - y_k}{\sqrt{(x_u-x_k)^2+(y_u-y_k)^2}}$, and $\sin(\xi_{k,u}^{RG}) = \frac{x_u - x_k}{\sqrt{(x_u-x_k)^2+(y_u-y_k)^2}}$ with $\phi_{k,u}^{RG}$ and $\xi_{k,u}^{RG}$ denoting the vertical and horizontal angles of departure (AoD) between the k-th user and the u-th AIRS.

Therefore, the effective channel gain of the k-th user for the i-th subcarrier is defined as

$$c_{k,i} = \left| h_{k,i}^{BG} + \left(h_{k,u,i}^{RG}\right)^H \Theta_u h_{u,i}^{BR} \right|^2, \tag{9}$$

where $c_{k,i}$ includes the random component of the NLOS channel and is a random variable. Based on the relevant discussion in [12], the expected value of $c_{k,i}$ and the corresponding signal to noise ratio (SNR) can be written as

$$\mathbb{E}\{c_{k,i}\} = \left| \hat{h}_{k,i}^{BG} + \left(\hat{h}_{k,u,i}^{RG}\right)^H \Theta_u h_{u,i}^{BR} \right|^2 + \frac{\beta - k_1}{(d_k^{BG})^\alpha} + \frac{M\beta(\beta - k_2)}{\left(d_{k,u}^{RG}\right)^{\alpha'} \left(d_u^{BR}\right)^2}, \tag{10}$$

$$\text{SNR}_{k,i} = \frac{p_{k,i}\,\mathbb{E}\{c_{k,i}\}}{\sigma^2}, \tag{11}$$

where $p_{k,i}$ is the power allocated to user k on subcarrier i and $\sigma^2 = N_0\Delta f$ denotes the noise power on each subcarrier. The term $\mathbb{E}\{c_{k,i}\}$ denotes the mean of the effective channel power gain from the u-th AIRS to the k-th user, on the i-th subcarrier. In (10), two new channel components are introduced as

$$\hat{h}_{k,i}^{BG} = \sqrt{\frac{k_1}{\left(d_k^{BG}\right)^\alpha}}\,\bar{h}_{k,i}^{BG}, \tag{12}$$

$$\hat{h}_{k,u,i}^{RG} = \sqrt{\frac{k_2}{\left(d_{k,u}^{RG}\right)^{\alpha'}}}\,\bar{h}_{k,u,i}^{RG}, \tag{13}$$

where $k_1 = \frac{\mathcal{K}\beta}{1+\mathcal{K}}$ and $k_2 = \frac{\mathcal{K}'\beta}{1+\mathcal{K}'}$. The achievable user rate of user k is calculated as follows:

$$R_k = \sum_{i=1}^{I} s_{k,i} \log_2(1 + \text{SNR}_{k,i}), \tag{14}$$

where $s_{k,i}$ is a binary variable, equal to 1 if the subcarrier i is allocated to user k, and 0 otherwise.

III. Problem Formulation

Let $S = \{s_{k,i}, \forall k, i\}$, $\Theta = \{\Theta_u, \forall u\}$, $Q = \{q_u^R, \forall u\}$, and $P = \{p_{k,i}, \forall k, i\}$ represent the sets of decision variables for subcarrier assignment, AIRS phase shifts, AIRS placement, and power allocation respectively. Our objective is to maximize the sum rate of all users by jointly optimizing Q, Θ, S, and P. To this end, the optimization problem can be formulated as:

$$\max_{P,\Theta,S,Q} \sum_{k=1}^{K} R_k \tag{15}$$
$$\text{s.t.} \quad C1\colon\ s_{k,i} \in \{0,1\}, \forall k, i$$
$$C2\colon\ \sum_{k=1}^{K} s_{k,i} \le 1, \forall i$$
$$C3\colon\ p_{k,i} \ge 0, \forall k, i$$
$$C4\colon\ \sum_{k=1}^{K}\sum_{i=1}^{I} p_{k,i} \le P_{\max}$$
$$C5\colon\ R_k \ge R_{min}, \forall k$$
$$C6\colon\ 0 \le \theta_{u,m} < 2\pi, \forall u, m$$

In this problem, C1 ensures binary subcarrier allocation, and C2 guarantees that each subcarrier is allocated to at most one user to prevent interference. C3 enforces non-negative power allocation for all subcarriers and users. C4 imposes a limit on the total power budget across all users and subcarriers, ensuring that the sum does not exceed the maximum available power $P_{\max}$. C5 ensures fairness by guaranteeing that the achievable rate of each user meets or exceeds the minimum required rate $R_{\min}$. Finally, C6 constrains the AIRS phase shifts to lie within the range $[0, 2\pi)$, allowing precise signal reflection control. This optimization problem is a non-convex mixed-integer programming problem due to the coupling of binary variables S and the non-convex nature of the objective function and constraints such as C5. The binary nature of subcarrier allocation $s_{k,i}$ and the non-linear relationship between phase shifts and the objective further increase the complexity. To address this, we propose an iterative approach to find a suboptimal solution that balances computational efficiency and performance.

IV. Proposed Algorithm

In this section, we propose a methodology to solve the optimization problem efficiently. First, we associate each user with an AIRS using the K-means clustering algorithm. The location of each AIRS in the xy-plane is updated based on the average location of the users within its cluster. For simplicity, we assume a fixed altitude for all AIRS units, $z_u = H_0$, which defines the solution for Q. Next, we adopt a Block Coordinate Descent (BCD)-based iterative algorithm to solve the optimization problem. The problem is decomposed into two subproblems for the variables Θ and (P, S). In each iteration, one set of variables is optimized while the other is kept fixed. The iterations continue until convergence.

A. Optimizing the AIRS phase shift Θ

This optimization subproblem can be written as:

$$\max_{\Theta} \sum_{k=1}^{K} R_k \tag{16}$$
$$\text{s.t. } C5, C6.$$

where Θ represents the phase shift matrix of all the AIRS units. The problem is non-convex due to both the objective function and the constraint C5. To address this issue, we adopt a similar approach to the one in [5] and rewrite the first term of the expected channel as follows:

$$b_{k,u,i} \triangleq (\hat{h}^{RG}_{k,u,i})^H \ \mathrm{diag}\big(h^{BR}_{u,i}\big), \tag{17}$$

$$\left|\hat{h}^{BG}_{k,i} + (\hat{h}^{RG}_{k,u,i})^H \Theta_u h^{BR}_{u,i}\right|^2 = \left|\hat{h}^{BG}_{k,i} + b_{k,u,i}\,\theta_u\right|^2, \tag{18}$$

where $b_{k,u,i}$ is the cascaded BS-AIRS-User channel before the reconfiguration of AIRS. Based on (18), we denote $\bar{\bar{h}}^H_{k,u,i} = [\, b_{k,u,i}, \hat{h}^{BG}_{k,i}\,]$ and $v_u = [\theta_u^T, 1]^T$, and $\mathbb{E}\{c_{k,i}\}$ can be expressed as

$$\begin{aligned}\mathbb{E}\{c_{k,i}\} &= |\bar{\bar{h}}^H_{k,u,i} v_u|^2 + \frac{\beta - k_1}{(d^{BG}_k)^\alpha} + \frac{M\beta(\beta-k_2)}{(d^{RG}_{k,u})^{\alpha'}(d^{BR}_u)^2} \\ &= \mathrm{Tr}(H_{k,u,i} V_u) + \bar{\omega}_{k,u,i},\end{aligned} \tag{19}$$

where $H_{k,u,i} = \bar{\bar{h}}_{k,u,i}(\bar{\bar{h}}_{k,u,i})^H$, $\bar{\omega}_{k,u,i} = \frac{\beta-k_1}{(d^{BG}_k)^\alpha} + \frac{M\beta(\beta-k_2)}{(d^{RG}_{k,u})^{\alpha'}(d^{BR}_u)^2}$ and $V_u = v_u v_u^H$. Here, V_u is an $(M+1)\times(M+1)$ rank-one positive semidefinite matrix whose diagonal elements equal one. Let $V = \{V_u, \forall u\}$, then the sum rate of all users can be written as:

$$\begin{aligned}&R_{sum} \\ &= \sum_{k=1}^{K}\sum_{i=1}^{I} s_{k,i} \quad \left(\log_2\left(1 + \frac{p_{k,i}(\mathrm{Tr}(H_{k,u,i}V_u) + \bar{\omega}_{k,u,i})}{\sigma^2}\right)\right)\end{aligned} \tag{20}$$

Thus, the problem (16) can be written as:

$$\begin{aligned}&\min_V - R_{sum} \\ &\text{s.t. } C5,\ C7\colon [V_u]_{mm} = 1, m = 1,2,...,M+1 \\ &\quad C8\colon V_u \succeq 0, \quad V_u \in \mathbb{H}^{M+1} \\ &\quad C9\colon \mathrm{rank}(V_u) = 1.\end{aligned} \tag{21}$$

The constraint C9 is non-convex. Since V_u is Hermitian, we have:

$$\|V_u\|_* - \|V_u\|_2 = 0 \tag{22}$$

which can be added as a penalty term to the objective function:

$$\begin{aligned}&\min_V - R_{sum} + \zeta_v(\|V_u\|_* - \|V_u\|_2) \\ &\text{s.t. } C5, C7, C8\end{aligned} \tag{23}$$

where $\zeta_v > 0$ is the penalty coefficient and if $\zeta_v \to \infty$ the problem (23) becomes equivalent to (21). For the convex function $\|V_u\|_2$, a lower bound, $\underline{V_u}^{(n)}$, based on first-order Taylor expansion is given by:

$$\begin{aligned}\|V_u\|_2 \geq \underline{V_u}^{(n)} \triangleq \|{V_u}^{(n)}\|_2 + \\ \mathrm{Tr}\left[u_{\max}\left({V_u}^{(n)}\right)\left(u_{\max}\left({V_u}^{(n)}\right)\right)^H\left(V_u - {V_u}^{(n)}\right)\right]\end{aligned} \tag{24}$$

where $V_u^{(n)}$ is the given point at the n-th iteration of the algorithm and $u_{\max}(V_u^{(n)})$ denotes the eigenvector corresponding to the largest eigenvalue of $V_u^{(n)}$. Finally, the problem can be reformulated as:

$$\begin{aligned}&\min_V - R_{sum} + \zeta_v(\|V_u\|_* - \ \underline{V_u}^{(n)}) \\ &\text{s.t. } C5, C7, C8\end{aligned} \tag{25}$$

The problem (25) is convex and can be solved efficiently by the CVX solver. The summary of the proposed algorithm is shown in Algorithm 1.

Algorithm 1 Penalty-based Algorithm

```
Initialize V_u^(0), ∀u
repeat
    Set n = 0
    repeat
        Solve problem (25) for given V_u^(n)
        Update V_u^(n+1) with the solution and set n ← n + 1
    until Convergence or reaching maximum iterations
    Update V_u^(0) with obtained optimal solution and increment ζ_v
until Overall convergence or reaching maximum iterations
```

B. Joint Subcarrier and Power Allocation Optimization (S, P)

Optimizing subcarrier and power allocation simultaneously ensures more efficient utilization of network resources, particularly under stringent power and fairness constraints. For given $\{Q, \Theta\}$, the joint subproblem of subcarrier and power allocation, based on problem (15), can be formulated as

$$\begin{aligned}&\max_{P,S} \sum_{k=1}^{K} R_k \\ &\text{s.t. } C1, C2, C3, C4, C5.\end{aligned} \tag{26}$$

This problem represents a standard mixed-integer linear program (MILP), which can be efficiently addressed using the CVX-Mosek solver.

The solutions of these subproblems are integrated into the proposed algorithm, summarized in Algorithm 2. The algorithm begins with randomly initialized values for $V^{(0)}, P^{(0)}, S^{(0)}$, serving as input parameters. At each iteration, it alternates between optimizing V by applying Algorithm 1 while keeping P and S fixed and solving for P and S using CVX while holding V constant. This iterative process continues until the objective function no longer improves, and the solution that achieves the highest sum rate is selected as the final result.

Algorithm 2 Iterative Optimization Algorithm

```
Initialize V^(0), P^(0), S^(0)
Set r = 0
repeat
    Solve problem (25) using Algorithm 1 while keeping P^(r) and S^(r) fixed to obtain V^(r+1)
    Solve problem (26) to obtain P^(r+1) and S^(r+1) using CVX while keeping V^(r+1) fixed
    Compute new objective function value f^(r+1)
    Update r ← r + 1
until Convergence or reaching maximum iterations
Output: Final values V, P, S
```

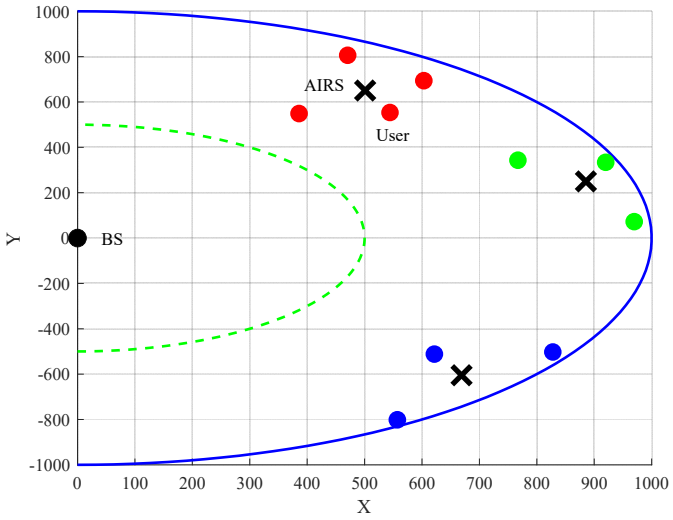

Fig. 2. Visualization of $U = 3$ AIRS and $K = 10$ user locations.

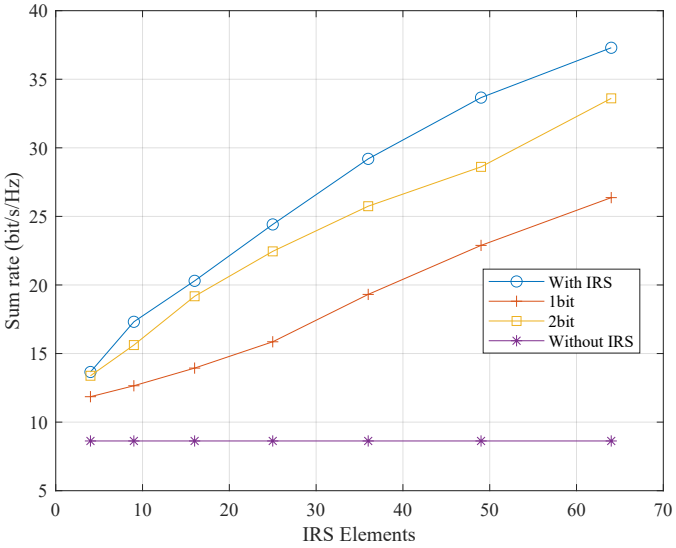

Fig. 3. Sum rate versus number of AIRS elements.

In Algorithm 1 (Step 3, V), the complexity arises from solving an SDP for U AIRS units, where each V_u is of size $(M+1) \times (M+1)$. With $m = O(U)$ constraints, the per-SDP complexity is $O(U^3 M^{3.5})$. Considering an inner loop of I_1 iterations and an outer loop of I_2 iterations, the overall complexity becomes $O(I_2 I_1 U^3 M^{3.5})$. In Step 4 (P, S), the mixed-integer optimization involves an $I \times K$ binary matrix S and power variables P, with complexity $O((IK)^{3.5})$ when solved using Mosek. With I_3 iterations in Algorithm 2, the total complexity is

$$O(I_3 \times \max(I_2 \times I_1 \times U^3 M^{3.5}, (I \times K)^{3.5})).$$

V. Numerical Results

To evaluate the proposed algorithm, we simulate an AIRS-assisted system in a semi-annular service area extending from 500 to 1000 meters from the BS with K users randomly distributed within the area. The BS is located at coordinates (0,0,30), where the z-coordinate represents the height in meters. AIRS units are deployed at a fixed altitude $H_0 = 120\ m$, the bandwidth is divided into $I = 64$ subcarriers, and we set $R_{min} = 0.5$ bit/s/Hz as the per-user QoS constraint. The maximum transmit power $P_{\max}$ and other relevant parameters are summarized in Table I.

Fig. 2 provides a visualization of the deployment scenario. The AIRS units are strategically positioned using the K-means clustering algorithm to serve users distributed within the service area. Fig. 3 illustrates the sum rate performance as a function of the number of AIRS elements for different quantization levels of the AIRS phase. The "With IRS" configuration achieves the highest sum rate, demonstrating the benefit of utilizing AIRS with optimal configurations. Quantized configurations (1-bit and 2-bit) show a slight reduction in performance due to the limited phase resolution. The "Without IRS" scenario serves as a baseline and highlights the significant performance improvements achieved with AIRS assistance.

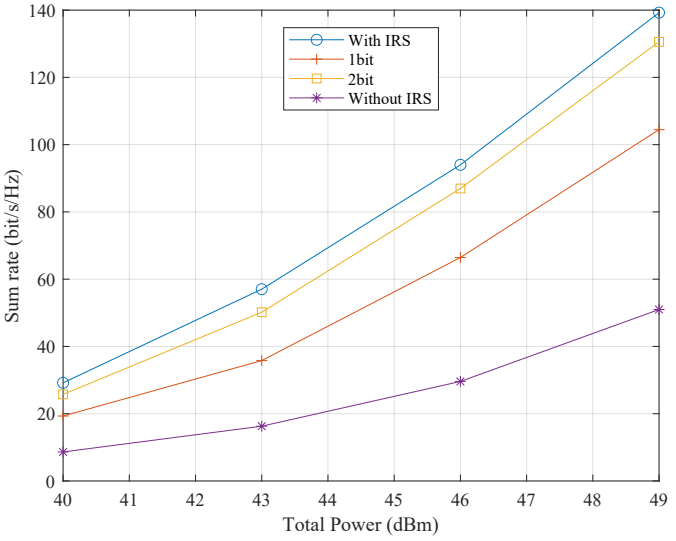

Fig. 4. Sum rate versus total transmit power for $M = 36$.

Fig. 4 presents the sum rate performance as a function of total transmit power for different system setups. The results demonstrate the effectiveness of AIRS-assisted communication in improving spectral efficiency. Notably, the sum rate increases significantly with the use of AIRS, particularly as the transmit power grows. The 2-bit quantization scheme outperforms the 1-bit scheme, demonstrating that finer phase resolution at the AIRS enhances performance, while AIRS-assisted schemes consistently outperform the non-IRS scenario, highlighting their potential in improving wireless communication systems under varying power budgets.

Fig. 5 shows the relationship between the average sum rate (bit/s/Hz) and the number of randomly located users. As the number of users increases, the average sum rate decreases because the bandwidth is shared among more users. The results show that the fully optimized AIRS achieves the highest

TABLE I
KEY SIMULATION PARAMETERS

Parameter	Description	Value	Parameter	Description	Value
K	Number of users	10	I	Number of subcarriers	64
U	Number of AIRS units	3	$P_{\max}$	Maximum transmit power	40 W
H_0	Height of AIRS units	120 m	N_0	Noise power spectral density	-169 dBm/Hz
Δf	Subcarrier spacing	15 kHz	f_c	Carrier frequency	3 GHz
$\mathcal{K}$	Rician factor for $h_{k,i}^{BG}$	5	$\mathcal{K}'$	Rician factor for $h_{k,u,i}^{RG}$	10
α	Path loss exponent for $h_{k,i}^{BG}$	4	α'	Path loss exponent for $h_{k,u,i}^{RG}$	2

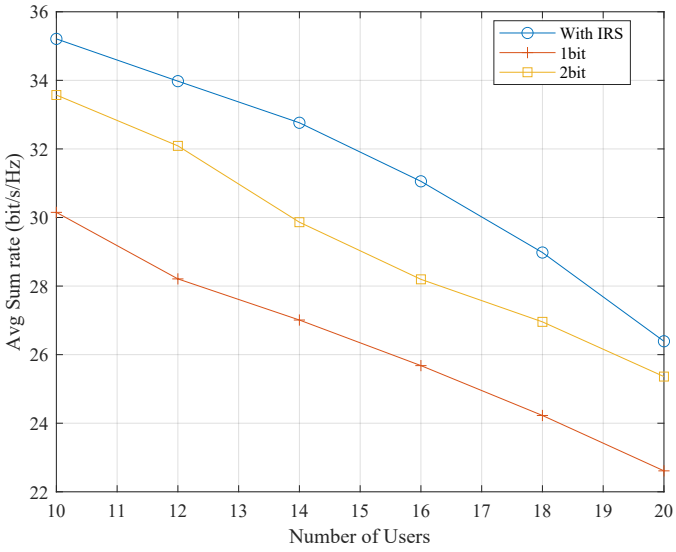

Fig. 5. Average sum rate (bit/s/Hz) versus number of users.

sum rate, and although phase quantization (1-bit and 2-bit) slightly reduces performance, it still provides significant gains compared to the non-IRS baseline.

VI. CONCLUSION

In this paper, we investigate the performance of AIRS-assisted communication systems by jointly optimizing resource allocation and system parameters. We demonstrate the significant potential of employing AIRS technology to enhance spectral efficiency and overall communication performance.

Our simulation results indicate that the inclusion of AIRS units consistently improves the sum rate compared to non-IRS setups, emphasizing their ability to provide robust coverage and support for higher data rates. Additionally, it is shown that higher quantization levels outperform lower ones, approaching the performance of ideal AIRS setups, while both clearly outperform the non-IRS scenario. Despite these promising results, several challenges remain, such as balancing system complexity and performance in large-scale deployments and addressing real-time resource optimization for dynamic environments. Future work should include developing simpler algorithmic solutions using heuristic and metaheuristic approaches, as well as solutions based on machine learning techniques.

REFERENCES

[1] Q. Wu and R. Zhang, "Towards smart and reconfigurable environment: Intelligent reflecting surface aided wireless network," *IEEE Commun. Mag.*, vol. 58, no. 1, pp. 106–112, 2020.

[2] M. Alzenad, A. El-Keyi, F. Lagum, and H. Yanikomeroglu, "3-d placement of an unmanned aerial vehicle base station (uav-bs) for energy-efficient maximal coverage," *IEEE Wireless Commun. Lett.*, vol. 6, pp. 434–437, 2017.

[3] G. Bansal, V. Chamola, B. Sikdar, and F. Yu, "Uav secaas: Game-theoretic formulation for security as a service in uav swarms," *IEEE Systems J.*, vol. 16, pp. 6209–6218, 2022.

[4] Q. Wu *et al.*, "Intelligent reflecting surface aided wireless communications: A tutorial," *IEEE Trans. Commun.*, vol. 69, no. 5, pp. 3313–3351, May 2021.

[5] Z. Wei, Y. Cai, Z. Sun, D. W. Kwan Ng, and J. Yuan, "Sum-rate maximization for irs-assisted uav ofdma communication systems," in *Proc. of IEEE GLOBECOM 2020 IEEE Global Commun. Conf.*, 2020, pp. 1–7.

[6] X. Mu, Y. Liu, L. Guo, J. Lin, and H. V. Poor, "Intelligent reflecting surface enhanced multi-uav noma networks," *IEEE J. Select. Areas Commun.*, vol. 39, no. 10, pp. 3051–3066, 2021.

[7] X. Pang, M. Sheng, N. Zhao, J. Tang, D. Niyato, and K. Wong, "When uav meets irs: Expanding air-ground networks via passive reflection," *IEEE Wireless Commun.*, vol. 28, pp. 164–170, 2021.

[8] Y. Qian, C. Yang, Z. Mei, X. Zhou, L. Shi, and J. Li, "On joint optimization of trajectory and phase shift for irs-uav assisted covert communication systems," *IEEE Trans. Veh. Technol*, vol. 72, no. 10, pp. 12 873–12 883, 2023.

[9] G. Iacovelli, A. Coluccia, and L. A. Grieco, "Multi-uav irs-assisted communications: Multinode channel modeling and fair sum-rate optimization via deep reinforcement learning," *IEEE Internet Things J.*, vol. 11, no. 3, pp. 4470–4482, 2024.

[10] H. Nguyen-Kha, H. V. Nguyen, M. T. P. Le, and O.-S. Shin, "Joint uav placement and irs phase shift optimization in downlink networks," *IEEE Access*, vol. 10, pp. 111 221–111 231, 2022.

[11] M.-H. T. Nguyen, E. Garcia-Palacios, T. Do-Duy, O. A. Dobre, and T. Q. Duong, "Uav-aided aerial reconfigurable intelligent surface communications with massive mimo system," *IEEE Trans. Cogn. Commun. and Netw.*, vol. 8, no. 4, pp. 1828–1838, 2022.

[12] X. Mu, Y. Liu, L. Guo, J. Lin, and H. V. Poor, "Intelligent reflecting surface enhanced multi-uav noma networks," *IEEE J. Select. Areas Commun.*, vol. 39, no. 10, pp. 3051–3066, 2021.